International Journal of Physics and Mathematical Sciences ISSN: 2277-2111 (Online)
An Online International Journal Available at http://www.cibtech.org/jpms.htm
2012 Vol. 2 (4) October-December, pp.17-26/ Patel et al.

Research Article

STRUCTURAL CHARACTERIZATION OF TUNGSTEN DISELENIDE SINGLE CRYSTAL

***CA Patel[1], Kaushik R Patel[2] and KD Patel[3]**
[1]Pilvai Science College, Pilvai (Gujarat)
[2]Biogas Research Center, Mahadev Desai Gramseva Mahavidhyalaya,
Gujarat Vidyapith, Sadra
[3]Department of Physics, Sardar Patel University, Vallabh Vidyanagar (Gujarat)
**Author for Correspondence*

ABSTRACT

The tungsten diselenide single crystals were grown by direct vapour transport (DVT) technique. The grown crystals were characterized with the help of Energy Dispersive Analysis by X-ray (EDAX), which gives the confirmation about the stoichiometry. The structural characterization was accomplished by X-ray diffraction (XRD) studies. The crystals are found to possess hexagonal structure. The lattice parameters, unit cell volume, particle size and X-ray density have been calculated for these crystals. The estimation of growth and deformation fault probabilities is calculated. The grown crystals were examined under optical zoom microscope for their surface topography study. The results obtained are discussed in detail.

INTRODUCTION

The transition metal dichalcogenides (including disulfide and diselenide) showed a wide variety of interesting physical properties, such as semiconducting, metallic, superconducting and magnetic behaviour (Boscher *et al.*, 2006; Tsuneta *et al.*, 2003; Salman *et al.*, 2007; Soto *et al.*, 2007 and Hu *et al.*, 2006). WSe_2 is an interesting member of the transition metal dichalcogenides family. It is a semiconductor with a band gap in the range of 1.2-2 eV, which is useful for photovoltaic and optoelectronic applications (Tiefenbacher *et al.*, 2000; Reshak *et al.*, 2007 and Reshak *et al.*, 2003). WSe_2 possess a layered structure with the metal atoms (W) bonded covalently between the layers of chalcogen atom (Se), and the remarkable feature of the WSe_2 is highly antiphotocorrosive due to the observation of layered structure, which makes it a strong candidate in the development of high efficiency photoelectrochemical solar cells (Devadasan *et al*., 2002).

In the past decades, the disulfides, such as MoS_2 and WS_2, had been extensively studied as lubrication additive on reducing friction and wear of rubbing pairs (Feldman *et al*., 1996 and Rapoport *et al*., 2002). The friction and wear mechanism had been discussed in details (Rappor *et al*., 1997; Rapoport *et al*., 2005; Rapoport *et al*., 1992; Chhowalla and Amaratunga G A J, 2000 and Sawyer *et al*., 1999).

Experiment

The single crystals of tungsten diselenide were grown by direct vapour transport technique. A highly pure compound of tungsten powder (purity: 99.99% make: Aldrich, USA) and selenide (99.98% Make: Aldrich, USA) were taken with stoichiometric proportion in the quartz ampoule for charge preparation. It was evacuated to a pressure of 10^{-5} torr and then sealed. This sealed ampoule was introduced into a two-zone furnace at a constant reaction temperature to obtain the charge. During the synthesis the temperature was slowly increased upto 1080ºC with 10ºC/hr. The ampoule was kept at 1080ºC temperature for 4 days. Then the furnace was slowly cooled (20ºC/hr) and brought to room temperature. The resulting brown and/or reddish charge was obtained in the ampoule. This charge was crushed and transferred to another quartz ampoule. After filling this charge evacuated it with 10^{-5} torr pressure and sealed it. This ampoule was placed in a dual zone horizontal furnace for 10 days with a temperature gradient shown in Table 1. After then furnace was cooled up to room temperature with a rate of 10ºC/hr. The entire material got converted into the form of crystals at the cooler end of the ampoule. The grown crystals were collected after breaking the ampoule. The optimum condition and physical parameters of as grown crystals are given in Table 1.

Table 1: Growth Conditions of WSe_2 single crystals used for next stage of work.

Crystals	**Ampoule Dimension**			**Temperature Distribution**			**Growth Time (Hours)**	**Crystals Dimension (mm^2)**
	Diameter (mm)		**Length (cm)**	**Source Zone (^0C)**	**Growth Zone (^0C)**	**Difference (^0C)**		
	Inner	**Outer**						
WSe_2	22	25	25	1080	1060	20	240	5– 6

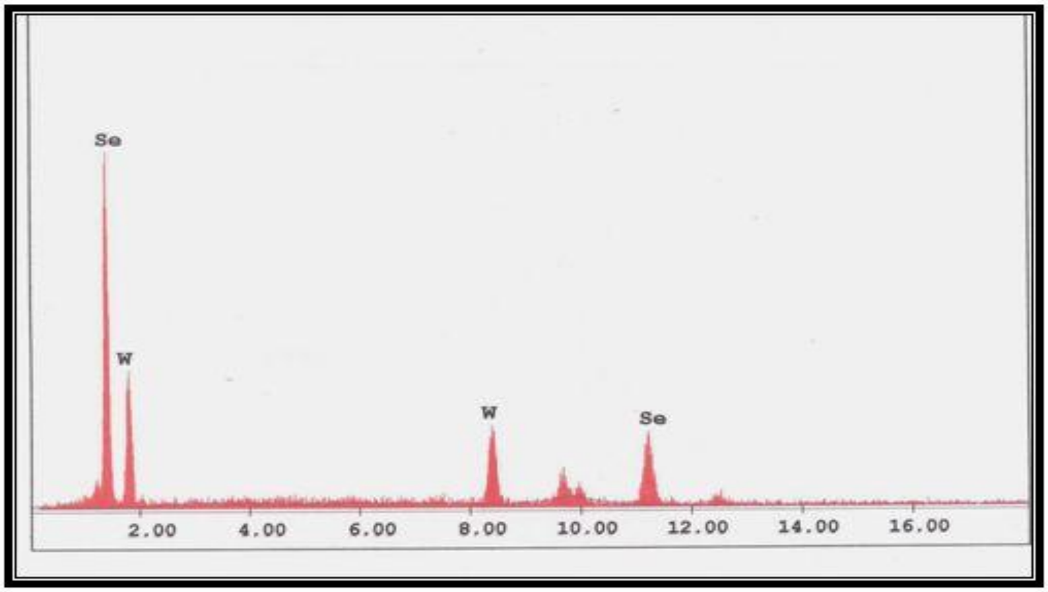

Figure 1: The energy dispersive spectra of the WSe_2 single crystals

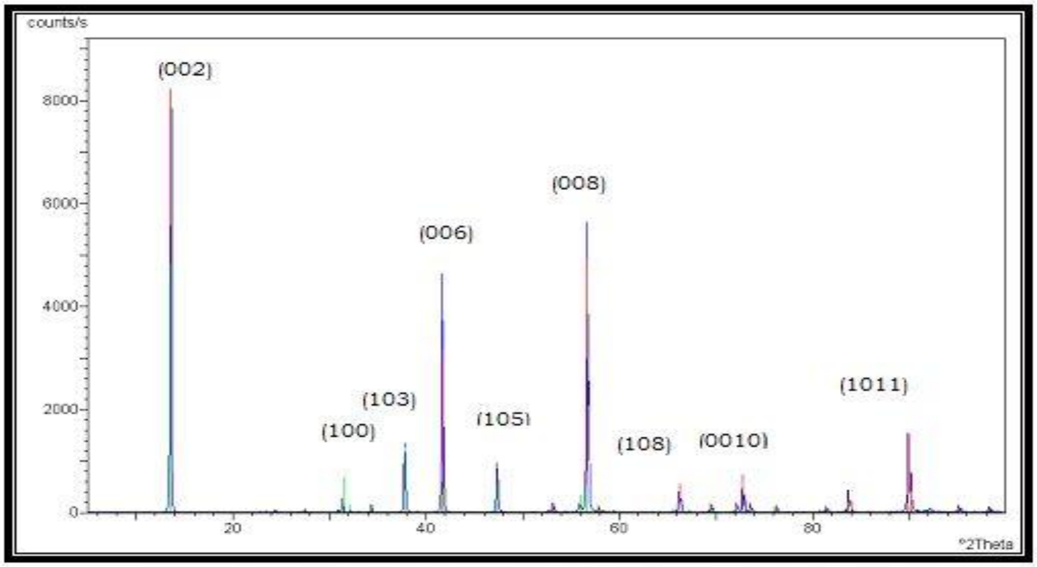

Figure 2: The X-ray diffractogram of WSe_2 single crystal

The EDAX of the grown WSe_2 single crystals in the present investigation was carried out using the electron microscope (Make: Phillips, Model: XL 30 ESEM). An energy dispersive spectrum taken from the representative samples of WSe_2 is shown in Figure 1.

The typical X-ray diffractogram of the grown WSe_2 single crystal is shown in Figure 2 was obtain with the help of Phillips X'pert MPD X-ray diffractometer employing CuK_α radiation. It has verified the phase and crystallanity of the compounds. In order to record the X-ray spectrum of each sample, synthesized product was crushed homogeneously with the help of mortar and pestle. The powdered sample was filled in a specially designed quartz sample holder. A thin pellet of the powder was formed by using hand pressure press. The X-ray diffractogram was recorded in the 2θ range of $3^0 - 100^0$ employing the wavelength $\lambda = 1.5405$ Å.

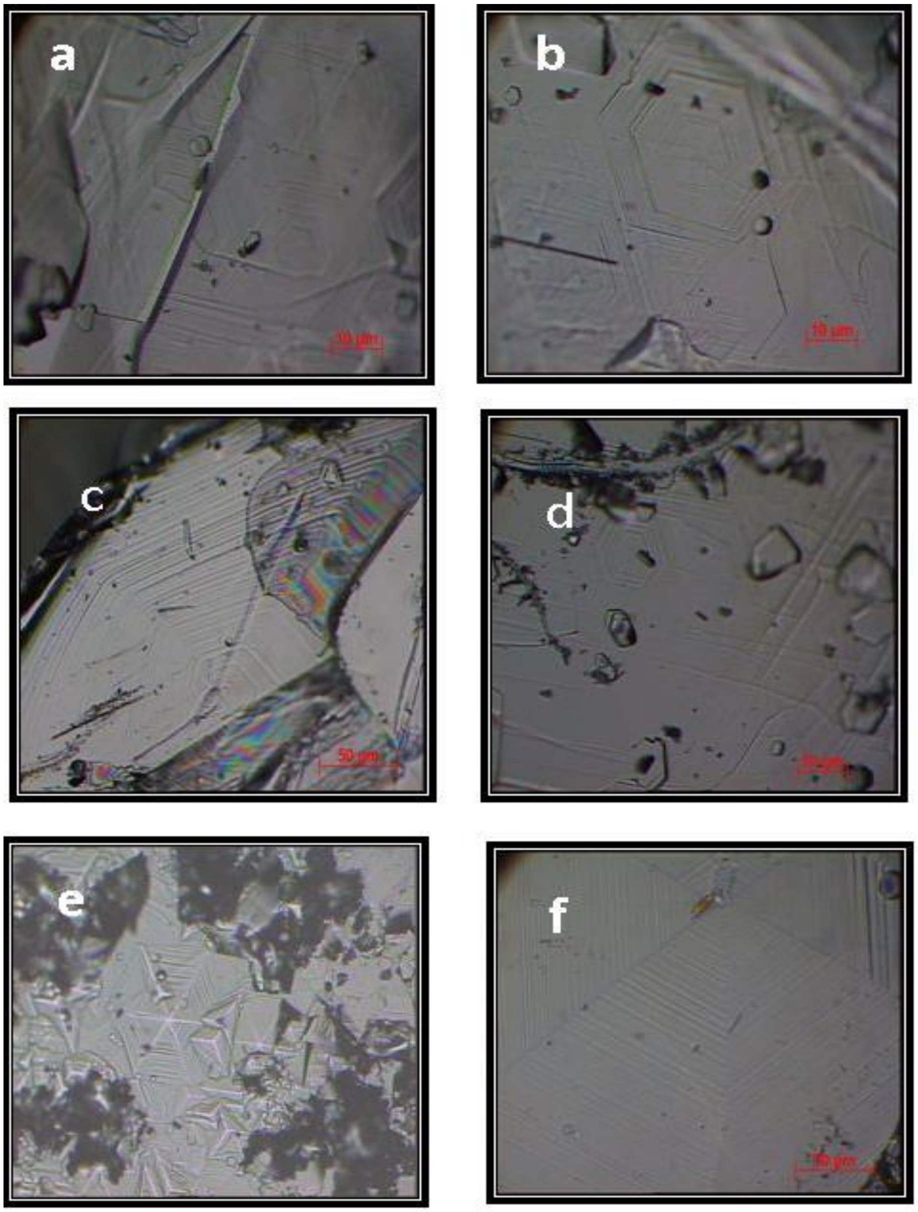

Figure 3: A typical spiral (Screw dislocation) on the as grown faces of WSe_2 crystals.

Close examination of the surface composed of layers helps a great deal in understanding the mechanism by which a crystal grows. Therefore, it was thought worthwhile to make surface characterization of these grown crystals by optical microscopy. The surface microstructure of as grown crystals were examined by computer added optical zoom microscope (Make: Carl Zeiss, Model Axiotech 100HD). The surface microstructure on the face of as grown crystals are shown in Figure 3, which shows layered surface structures.

RESULTS AND DISCUSSION

The Stoichiometric proportion of the constituent elements taken for the growth and data obtained from the EDAX are shown in Table 2, with chemical formula. The EDAX analysis shows that the grown crystals are stoichiometrycally perfect without any extra impurities.

Table 2: Chemical composition (wt. %) of as grown WSe_2 single crystals obtained by EDAX analysis with chemical formula.

Wt (%) of the elements	Stoichiometric proportion	Obtained from the EDAX	Chemical formula
Tungsten (W)	53.79	55.05	$W_{1.02}$
Selenium (Se)	46.21	44.95	$Se_{1.97}$

Table 3: Comparison of experimentally observed d-spacing of as- grown WSe_2 single crystals with JCPDS data sheet.

(h k l)	d- spacing (Å)	
	Experimental	JCPDS data
0 0 2	6.4994	6.4942
1 0 0	2.8455	2.8457
1 0 2	2.6061	2.6043
1 0 3	2.3773	2.3777
0 0 6	2.1630	2.1638
1 0 5	1.9176	1.9178
1 0 6	1.7218	1.7222
1 1 0	1.6425	1.6434
0 0 8	1.6222	1.6229
1 1 2	1.5922	1.5931
2 0 0	1.4234	1.4223
1 0 8	1.4100	1.4102
2 0 3	1.3523	1.3517
1 1 6	1.3090	1.3085
0 0 10	1.2988	1.299
1 0 9	1.2869	1.2867
2 0 5	1.2481	1.2475
1 0 10	1.1816	1.1808
1 1 8	1.1549	1.1545
1 0 11	1.0905	1.0903
2 1 3	1.0440	1.0439

Table 4: Observed and reported lattice parameters, unit cell volume, and X-ray density of the WSe_2 crystals from XRD data.

Parameters	Observed value	Reported value
a=b (Å)	3.28	3.280[6], 3.282[7], 3.278[8] 3.282[11], 3.286[12], 3.282[13] 3.285[2]
c (Å)	13.00	12.95[6], 12.96[9], 12.96[8] 12.98[2], 13.018[11], 12.976[12], 12.960[13]
Volume ($Å^3$)	121.04	120.66[6], 120.62[8]
X-Ray density (gm/cm^3)	10.41	9.373[10]

In Figure 2, all the peaks were indexed with the help of "powder X" programme. The respective diffractograms contain 41 sharp lines of varying intensities for WSe_2. The highest intensity peak indicates the most preferred orientation (given in Table 3) of the crystal grains. The analytical indexing of the pattern thus obtained was done to calculate the lattice parameters for the hexagonal layered structures. The results obtained for as grown crystals of WSe_2 are given in Table 4. In order to affirm that these lines belong to tungsten diselenide, the d spacing and relative intensities of these lines were compared with JCPDS data 2H-WSe_2 polytypes [JCPDS data (WSe_2, 1997)].

It is noted that 21 of WSe_2 d spacing of JCPDS data match with the present diffractogram. For each peak in the diffractogram, the d-values corresponding to different h k l planes were evaluated from the respective diffractograms and are given in the Table 3. The evaluated d-values were compared with the JCPDS files [JCPDS data (WSe_2, 1997)]. However relative intensities do show deviations.

It may be further noted that the lines which are still left are of very low intensity in as grown crystals and these may be considered as a part of the background. Matching of the observed d-values and the standard JCPDS data infers that the grown materials possess hexagonal structure having $P6_3/mmc$ space group.

The lattice parameters for the hexagonal structure have been computed, using the equation (1), i.e.

$$\frac{1}{d^2} = \frac{4}{3}\left(\frac{h^2 + hk + k^2}{a^2}\right) + \frac{l^2}{c^2} \tag{1}$$

where d is the inter planar spacing obtained from the diffractogram, h, k, l are the miller indices and a & c are the unit cell dimensions. Substituting the values of inter planar spacing parameter d corresponding to the planes having index {00l}, the value of lattice the parameter 'c' has been determined. Substituting the value of c and d for the rest of the planes, lattice parameters for rest of all the planes have been calculated. The values of the computed lattice parameters for all the compounds in present investigation are shown in Table 4. The calculated values are in good agreement with that reported in the JCPDS X-ray powder diffraction data base [JCPDS data (WSe_2, 1997)]. Using the values of lattice parameters a, b, c the unit cell volume (V) has been calculated with the help of the equation (8). It is found that there is no significant variation in the values of lattice parameters a and c.

The density ρ of the grown crystals was calculated by the formula,

$$\rho = \frac{\sum A}{VN} \tag{2}$$

Where, ΣA is the total weight of the atoms in the unit cell = MZ. Here M is the molecular weight and Z is the number of molecules/unit cell, N is the Avogadro number and V is the unit cell volume. The quadratic form of the Bragg equation for a Hexagonal system, of MX_2 is given as (Cullity, 1978 and Suryanarayana, 1998).

$$\frac{1}{d^2} = \frac{4}{3}\left(\frac{h^2 + hk + k^2}{a^2}\right) + \frac{l^2}{c^2} \tag{3}$$

This equation can be set up in terms of $\sin^2\theta$ rather than d, by combining with the Bragg's law

$$\frac{1}{d^2} = \frac{4}{3}\left(\frac{h^2 + hk + k^2}{a^2}\right) + \frac{l^2}{c^2} = \frac{4\sin^2\theta}{\lambda^2} \qquad (4)$$

This may be written in the form

$$\sin^2\theta = \frac{\lambda^2}{4}\left[\frac{4}{3}\left(\frac{h^2 + hk + k^2}{a^2}\right) + \frac{l^2}{c^2}\right] \qquad (5)$$

or

$$\sin^2\theta = \frac{\lambda^2}{4a^2}\left[\frac{4}{3}\left(h^2 + hk + k^2\right) + \frac{l^2}{\left(c/a\right)^2}\right] \qquad (6)$$

Volume, in terms of lattice constants *a, b, c* and angles α, β, γ is given as

$$V^2 = a^2b^2c^2\left(1 - \cos^2\alpha - \cos^2\beta - \cos^2\gamma + 2\cos\alpha - \cos\beta - \cos\gamma\right) \qquad (7)$$

For hexagonal system, $\alpha = \beta = 90^0$, $\gamma = 120^0$ and $a = b \neq c$,
Substituting above values in equation (7), the unit cell volume is given as,

$$V = \frac{\sqrt{3}}{2}\ a^2c\ (\text{Å})^3 = 0.866\ a^2c\ (\text{Å})^3 \qquad (8)$$

The values of lattice parameters *a* (Å), *b* (Å), *c* (Å), X-ray density (ρ) and unit cell volume (*V*) (Å^3) obtained from the diffraction data for as grown crystals of WSe_2 and compared with the reported data. The observed and reported lattice parameters of as grown crystals given in Table 4 are in good agreement with reports observed in literature [JCPDS data (WSe_2, 1997; Deshpande *et al*., 1999; Tomm and Fiechter, 2005 and Sharma *et al*., 1999).

Particle Size Determination

Table 5: XRD data entry of the WSe_2 single crystals and particle size determination.

(h k l)	d-spacing (Å)	Angle 2θ (Degree)	Peak intensity (Counts/sec)	Tip width ($\beta_{2\theta}$)	Particle size (Å)
0 0 2	6.4994	13.61	8357.23	0.18	565.94
1 0 0	2.8455	31.41	302.10	0.18	490.63
1 0 2	2.6061	34.38	142.55	0.18	5534.83
1 0 3	2.3773	37.81	1149.16	0.18	491.38
0 0 6	2.1630	41.72	3133.96	0.18	1152.73
1 0 5	1.9176	47.36	766.58	0.18	4165.56
1 0 6	1.7218	53.14	165.92	0.24	2763.75
1 1 0	1.6425	55.93	163.25	0.24	386.30
0 0 8	1.6222	56.69	4911.65	0.24	368.89
1 1 2	1.5922	57.86	82.80	0.24	464.23
2 0 0	1.4234	65.52	50.92	0.18	2182.63
1 0 8	1.4100	66.72	549.79	0.24	1009.05
2 0 3	1.3523	69.44	177.82	0.18	497.17
1 1 6	1.3090	72.09	177.82	0.18	5895.57
0 0 10	1.2988	72.74	682.10	0.18	2049.92
1 0 9	1.2869	73.53	173.35	0.18	825.23
2 0 5	1.2481	76.21	131.41	0.24	400.51
1 0 10	1.1816	81.37	100.19	0.18	496.63
1 1 8	1.1549	83.66	422.76	0.18	893.22
1 0 11	1.0905	89.88	1521.69	0.18	852.67
2 1 3	1.0440	95.08	134.17	0.12	804.59

In order to obtain an idea about the particle size distribution in WSe_2 single crystals, the particle size was calculated using Scherrer's formula (Al-Hilli and Evans, 1972) given as

$$\mathrm{t}=\frac{k\lambda}{\beta_{2\theta}\cos\theta} \tag{9}$$

Where t is the crystallite thickness as measured perpendicular to the reflecting plane; k is Scherrer's constant whose value is chosen as unity assuming the particle to be spherical; λ(1.5405 Å) is the wavelength of the X-ray radiation, $\beta_{2\theta}$ is the width at half the maximum intensity measured in radians, and θ_0 is the Bragg angle. Table 5 records the crystallite size for WSe_2 single crystals.

The particle size of as grown crystals is found to be in the range of 30nm – 600nm as shown in Table 5.

The intense and sharp peaks reveal the excellent crystallinity of the products and confirm their stoichiometric nature. The reflections corresponding to the observed peaks indicate the formation of single-phase material.

Estimation of Growth and Deformation Fault Probabilities

Perfect crystalline structure is an ideal concept since perfect crystals are neither available in nature nor can be grown in the laboratory. Several types of defects are always present in crystal e.g. point defects, stacking fault etc. The study of stacking fault is very important because it plays a fundamental role in the description of defects. The enhanced conduction of the stacking faults along the c-axis is difficult to understand because of the extreme two-dimensional character of the MX_2 layer compounds. The only way to understand this conduction is by supposing the presence of stacking faults in these crystals (Vora, 2007). The structure of MX_2 type layers consists of planes of hexagonally close packed chalcogen atoms (X) inter-linked with planes of metal atoms (M) (also on hexagonal sites) to give a stacking sequence A_B B_A A_B B_A…. where "A_B" is hexagonal X-M-X layer with 'X' atoms in 'A' positions and 'M' atoms in 'B' positions, "B_A" is a layer with 'X' atoms in 'B' positions and 'M' atoms in 'A' positions. Stacking faults may arise from various types of dissociated or undissociated basal dislocations an example of which would be $A_B B_A A_C C_A$….

Warren (1959) has shown that in case of hexagonal close packed metals, it is possible to make a realistic estimation of the deformation fault probability 'α' and the growth fault probability 'β' by measuring the half width of X-ray diffraction lines. Reflections for which h-k=3n, where 'n' is an integer, are independent of stacking faults, whereas reflections for which h-k=3n ± 1 and $l \neq 0$ depend upon the stacking faults in the crystal structure. An estimation of the deformation and growth fault probability can be obtained from the (*hkl*) values using following formulae.

$$\left(3\alpha+3\beta\right)=\frac{B_{2\theta}\times\pi^{2}\times c^{2}}{360\times l\times d^{2}\times\tan\theta} \qquad \text{for ` } l \text{ ' even} \tag{10}$$

$$\left(3\alpha+\beta\right)=\frac{B_{2\theta}\times\pi^{2}\times c^{2}}{360\times l\times d^{2}\times\tan\theta} \qquad \text{for ` } l \text{ ` odd} \tag{11}$$

where $B_{2\theta}$ is the full width at half the maximum intensity expressed in degrees, $c = 2d_{002}$, '*l*' is the Miller index in the (*h k l*) plane, α and β are the deformation fault probability and the growth fault probabilities respectively. '*d*' is the inter planer spacing for (*h k l*) reflection in question, θ is the Bragg angle corresponding to this (*h k l*) plane.

The input parameters, which are taken from the X-ray diffractogram for WSe_2 single crystals are depicted in Table 6.

From equations (10) and (11), it is clear that by measuring half width $B_{2\theta}$ for reflections with both even and odd values of 'l', it is possible to calculate the stacking fault probabilities α and β.

The half widths of the reflections from the stacking faults have been calculated by eliminating the effects of small domain size and strain by taking the nearest fault-free reflections. For the estimation of α and β of as grown WSe_2 single crystals, the following X-ray reflections (002), (102), (106), (103), (213) and (203) were used. The calculated values of α and β are given in Table 7.

Table 6: Estimation of stacking (deformation and growth) fault probability of as grown WSe_2 single crystals.

Crystal	(h k l)	3α + 3β	3α + β	α	β
WSe_2	0 0 2	0.001584	-	0.03382	-0.03350
	1 0 2	0.000507	-		
	1 0 6	0.000777	-		
	1 0 3	-	0.082284		
	2 1 3	-	0.035778		
	2 0 3	-	0.085861		

Table 7: The Number of deformation and growth faults for 1000 atomic layers of WSe_2.

As grown crystals	Deformation fault (α)	Growth fault (β)
WSe_2	33.82	33.50

From the Table 7, it can be seen that there is a significant variation shown in the deformation fault probability (α) and growth fault probability (β) may be due to small off-stoichiometry as observed by EDAX. The opposite sign of both probabilities indicates that the created stacking fault is an intrinsic type in WSe_2 crystals, because existence of stacking fault leads to a localization of electron states. The calculations of the stacking faults may be considered as one of the guidelines for further detailed study of defects and various properties of crystals.

Microstructural Properties of the Grown Crystals

The crystals grown in present investigations have been found to possess flat faces whose surface topographic studies were carried out. Study of microstructures reveals a large number of crystallographically oriented spirals on the grown faces of these crystals, which suggests a screw dislocation mechanism is involved in the growth of these crystals (Warren, 1959). In general, presence of screw dislocations in grown crystals shows the characteristic property of the growth from gaseous phase. The pattern of growth spirals, both with unique or with multiple burger vectors strongly depends on the rate of movement of dislocations and atomic steps in different crystallographic directions relative to the faces. Further, the feature of polygonized spirals reflects the symmetry of that face of the crystal and the formation develops perpendicular to the direction of crystal growth. Thus the peculiarities of the growth of faces are directly reflected with the distinctive features of the growth conditions. Figure 3(a-b) of WSe_2 crystal depicts the initiation and the advancement of growth spirals originating from a point and gives a clear view of the left handed (Clockwise) growth spirals on the surface (Agarwal *et al.*, 1980 and Bletskan, 2006).

During the course of our investigations, we sometimes have come across certain regions on the grown WSe_2 crystal faces where hexagonal and triangular features were present on the same face (Figure 3 e). Since the morphology of the growth features follows the symmetry of the crystal structure, a triangular feature clearly belongs to a rhombohedral polytype and a hexagonal feature to a hexagonal polytype (Agarwal *et al.*, 1989 and Agarwal *et al.*, 1979). Figure 3(c-d) shows the co-existence of 2H + 3R polytypes on the same crystal. Since the positions in which this co-existence is seen are very rare, one can say that our crystals of WSe_2 are primarily 2H type but traces of 3R type are also present. This can also be verified from the a-axis oscillation photograph. From literature survey (Agarwal *et al.*, 1980) and analyses of our crystals, it is seen that there is coexistence of 2H and 3R polytypes on the same crystal.

But the amount of 3R phase is very small, thus confirming the crystal is 2H polytype predominantly. This result is a re-confirmation of the conclusions drawn from the d-values obtained in XRD.
The common features observed were regular polygonal hexagonal spirals (Agarwal *et al*., 1981). In all of the above Figures 3(a-e), it can be seen that the surfaces are not very clean from viewpoint of hexagonal or triangular features. This is mainly because of the fact that the photographs of all these crystals were taken prior to giving any surface cleaning treatment (i.e. directly after growth with as grown surfaces). These surfaces can be made smoother by giving some chemical treatment. Also, the cleaving of samples will reduce such non-uniformities as the inner layer surfaces are expected to have better growth features shown in Figure 3(f).

CONCLUSION

EDAX analysis of the as grown crystals shows that they are stoichiometrically perfect.
X-Ray diffraction analysis of these crystals shows that these crystals possess hexagonal structure.
The lattice parameters are very well matched with the value obtained by earlier workers.
Particle sizes for some (h k l) planes of the as grown crystals are found.
Deformation and Growth fault probability are found, which shows the layer structure defects of as grown crystals.
Optical microscopy shows that a typical spiral, point crack, microcrystal, mixer of triangular and hexagonal features on the WSe_2 crystal structure and finally cleaved surface with hexagonal growth pattern.

REFERENCE

Agarwal MK, Patel HB and Nagireddy K (1979). *Indian Journal of Physics* **53A** 349.
Agarwal MK, Patel HB and Patel JV (1980). *Crystal and Technique* **15**(7) 769.
Agarwal MK, Rao VV and Pathak VM (1989). Photoelectrochemical solar cell fabrication with tungsten diselenide single crystals. *Bulletin of Material Science* **12**(2) 163.
Agarwal MK, Wani PA and Patel JV (1981). *Crystal Research and Technology-Journal* **16**(8) 899.
Agarwal MK, Rao VV and Pathak VM (1989). Growth of n-type and p-type WSe_2 crystals using $SeCl_4$ transporter and their characterization. *Journal of Crystal Growth* **97**(3-4) 675-679.
Al-Hilli AA and Evans BL (1972). The preparation and properties of transition metal dichalcogenide single crystals. *Journal of Crystal Growth* **15** 93-101.
Bletskan DI (1979). *Ukrainskii Fizichnii Zhurnal* **24**(9) 1321.
Bletskan DI (2006). *Journal of Ovonic Research* **2** 137.
Boscher ND, Carmalt CJ and Parkin IP (2006). Atmospheric pressure chemical vapor deposition of WSe_2 thin films on glass—highly hydrophobic sticky surfaces. *Journal of material chemistry* **16** 122.
Boscher ND, Carmalt CJ and Parkin IP (2006). Atmospheric Pressure Chemical Vapour Deposition of $NbSe_2$ Thin Films on Glass. *Europian Journal of Inorganic Chemistry* **10** 1255-1259.
Chhowalla M and Amaratunga GAJ (2000). Thin films of fullerene-like MoS_2 nanoparticles with ultra-low friction and wear. *Nature* **60** 164.
Cullity BD (1978). *Elements of X-ray diffraction.* (Addision-Wesley, USA) **2** 189.
Deshpande MP, Patel PD, Vashi MN and Agarwal MK (1999). Effect of intercalating indium in WSe_2 single crystals. *Journal of Crystal Growth* **97**(4) 833-840.
Devadasan J Jebaraj, Saneeviraja C and Jayachandran M (2002). *Materials Chemistry and Physics - Journal* **77** 397.
Feldman Y, Frey GL, Homyounfer M and Tenne RJ (1996). *The Journal of the American Chemical Society* **118**(24) 5632.
Hu SY, Lee YC, Shen L, Chen KW, Tiong KK and Huang YS (2006). Temperature dependence of absorption edge anisotropy in 2H- $MoSe_2$ layered semiconductors. *Solid State Communications* **139**(4) 176-180.

JCPDS(1997). *International Centre for Diffraction Data*, PDF-2 File No. 38-1388 (WSe_2).

Rapoport L, Leshchinsky V, Lvovsky M, Lapsker I, Volovik Yu and Tenne R (2002). *Tribology International* **35** 47.

Rapoport L, Nepomnyashchy O, Lapsker I, Verdyan A, Soifer Y, Popovitz R -Biro and Tenne (2005). Behavior of fullerene-like WS2 nanoparticles under severe contact conditions. *Wear* **259** 703-707.

Rapoport L, Nepomnyashchy O, Lapsker I, Verdyan A, Soifer Y, Popovitz-Biro R and Tenne (2005). Friction and wear of fullerene-like WS_2 under severe contact conditions: friction of ceramic materials. *Tribology Letters* **19**(2) 143-149.

Rappor L, Bilik Y, Feldman Y, Homyounfer M, Cohen SR and Tenne R (1997). Hollow nanoparticles of WS_2 as potential solid-state lubricants. *Nature* **387** 791-793.

Reshak Ali Hyssain and Auluck Sushil (2003). Electronic and optical properties of 2*H*-WSe_2 intercalated with copper. *Physical Review B* **68** 195107.

Reshak Ali Hyssain and Auluck Sushil (2007). The linear and nonlinear optical properties of WS_xSe_{2-x} (x=0.5, 1.5, and 2.0) *Physica B* **393**(1-2) 88-93.

Salman Z, Wang D, Chow KH, Hossain MD, Kreitzman SR, Keeler TA, Levy CDP, MacFarlane WA, Miller RI, Morris GD, JParolin T, Saadaou H, Smadella M and Kiefl RF (2007). Magnetic-Field Effects on the Size of Vortices below the Surface of $NbSe_2$ Detected Using Low Energy β-NMR. *Physical Review Letter* **98**(16) 167001–167004.

Sawyer WG, Thierry A and Blanchet TA (1999). Lubrication of Mo, W, and their Alloys with H_2S gas admixtures to room temperature air. *Wear* **225** 581.

Sharma S, Ambrosch-Draxl C, Khan MA, Blaha P and Auluck S (1999). Optical properties and band structure of 2*H*-WSe_2. *Physical Review B* **60**(12) 8610.

Soto F, Berger H, Cabo L, Carballeira C, Mosqueira J, Pavuna D, Toimil P and Vidal F (2007). Electric and magnetic characterization of $NbSe_2$ single crystals: Anisotropic superconducting fluctuations above $T_{C.}$ *Physica C* **460** 789.

Suryanarayana C and Norton Grant M (1998). X-ray diffraction a practical approach. (Plenum Press, New York) **125.**

Tenne R, Margulis L, Genut M and Hodes G (1992). Polyhedral and cylindrical structures of tungsten disulphide. *Nature* **60** 444-446.

Tiefenbacher KS Eyert V Pettenkofer C and Jaegermann W (2000). Electronic properties of WS_2 monolayer films. *Thin Solid Film* **380**(1-2) 221-223.

Tomm Y and Fiechter S (2005). Crystal growth of materials for photovoltaics. *Journal of Ceramic Processing Research* **6**(2) 141-145.

Tsuneta T, Toshima T, Inagaki K, Shibayama T, Tanda S, Jui S, Ahlslog M, Harkonen P and Paalanen (2003). Formation of metallic $NbSe_2$ nanotubes and nanofibers. *Current Applied Physics* **3**(1) 473-476.

Vora AM (2007). Effect of indium intercalation on various properties of $MoSe_2$ single crystals. *Crystal Research and Technology Journal* **42** 286-289.

Warren BE (1959). *Progress in Metal Physics- Journal* **8** 147.

Zhou Z, Jin R, Eres G, Mandrus D, Barzykin V, Sclottmann P, Hor YS, Xiao Z and Mitchell JF (2007). Resistance and current-voltage characteristics of individual superconducting $NbSe_2$ nanowires. *Physics Review B* **76** 104511.